

D semileptonic form factors and $|V_{cs(d)}|$ from 2+1 flavor lattice QCD

**Jon A. Bailey^{*a,b}, A. Bazavov^c, A.X. El-Khadra^d, Steven Gottlieb^e, R.D. Jain^d,
A.S. Kronfeld^a, R.S. Van de Water^c, and R. Zhou^e**

Email: jabailey@fnal.gov

^aTheoretical Physics Department, Fermilab, Batavia, IL 60510, USA

^bDepartment of Physics and Astronomy, Seoul National University, Seoul, 151-747, ROK

^cDepartment of Physics, Brookhaven National Laboratory, Upton, NY 11973, USA

^dPhysics Department, University of Illinois, Urbana, IL 61801, USA

^eDepartment of Physics, Indiana University, Bloomington, IN 47405, USA

Fermilab Lattice and MILC Collaborations

The measured partial widths of the semileptonic decays $D \rightarrow K\ell\nu$ and $D \rightarrow \pi\ell\nu$ can be combined with the form factors calculated on the lattice to extract the CKM matrix elements $|V_{cs}|$ and $|V_{cd}|$. The lattice calculations can be checked by comparing the form factor shapes from the lattice and experiment. We have generated a sizable data set by using heavy clover quarks with the Fermilab interpretation for charm and asqtad staggered light quarks on 2+1 flavor MILC ensembles with lattice spacings of approximately 0.12, 0.09, 0.06, and 0.045 fm. Preliminary fits to staggered chiral perturbation theory suggest that we can reduce the uncertainties in the form factors at $q^2 = 0$ to below 5%.

XXIX International Symposium on Lattice Field Theory

July 10-16 2011

Squaw Valley, Lake Tahoe, California

^{*}Speaker.

1. Introduction

Performing a global fit under the assumption of a unitary CKM matrix [1] yields precise values for $|V_{cs}|$ and $|V_{cd}|$ [2]. If new physics in flavor introduces deviations from unitarity, however, values of the CKM matrix elements from direct determinations will in general differ from those predicted by the global fit. Moreover, improving tests of second row and column unitarity requires improved direct determinations of $|V_{cs}|$ [2].

In the limit of massless leptons, the rates for the semileptonic decays $D \rightarrow K(\pi)\ell\nu$ become¹

$$\frac{d\Gamma(D \rightarrow K(\pi)\ell\nu)}{dq^2} = \frac{G_F^2}{24\pi^3} |\mathbf{p}_{K(\pi)}|^3 |V_{cs(d)}|^2 |f_+^{D \rightarrow K(\pi)}(q^2)|^2, \quad (1.1)$$

where $q^2 = (p_D - p_{K(\pi)})^2$, $\mathbf{p}_{K(\pi)}$ is the momentum of the $K(\pi)$ in the rest frame of the D , and $f_+^{D \rightarrow K(\pi)}(q^2)$ is defined in terms of the hadronic matrix element of the current $V_\mu = i\bar{s}\gamma_\mu c$ ($i\bar{d}\gamma_\mu c$):

$$\langle K(\pi)|V_\mu|D \rangle = f_+^{D \rightarrow K(\pi)}(q^2) \left(p_D + p_{K(\pi)} - \frac{m_D^2 - m_{K(\pi)}^2}{q^2} q \right)_\mu + f_0^{D \rightarrow K(\pi)}(q^2) \frac{m_D^2 - m_{K(\pi)}^2}{q^2} q_\mu. \quad (1.2)$$

Given the normalization of the form factors $f_+^{D \rightarrow K(\pi)}(q^2)$ from lattice QCD, the CKM matrix elements $|V_{cs(d)}|$ can be extracted from experimental measurements of the branching fractions.

Agreement with the Standard Model values provides important validation of our methods, which we also use to calculate the form factors for $B \rightarrow \pi\ell\nu$ [4] and $B \rightarrow K\ell^+\ell^-$ [5]. Both decays are central in searches for new physics; the former allows direct extraction of $|V_{ub}|$, while the latter is loop-suppressed in the Standard Model. New physics seems unlikely to enter the tree-level decays $D \rightarrow K(\pi)\ell\nu$ before the B decays. The Fermilab method applies to charm and bottom, so consistency between our D form factors and the normalizations implied by the global fit is direct evidence of our ability to precisely extract the B form factors.

2. Method

For the up, down, and strange quarks we use the asqtad-improved staggered action [6], for the charm quark we use the clover action with the Fermilab interpretation [7], and for the gluons we use a one-loop Symanzik improved gauge action [8]. We set the scale with f_π , tune the masses of the light quarks using the experimental values of m_π and m_K , and tune the hopping parameter of the charm quark with the spin-averaged kinetic mass of the D_s .

Table 1 summarizes our data set. We vary the valence light-quark masses on each ensemble from near the tuned strange mass m_s down to $\sim 0.1m_s$, and the lattice spacings from ≈ 0.12 fm to ≈ 0.045 fm. To increase statistics and reduce autocorrelations, we average over four source times and randomize the source spatial locations.

For calculations in the rest frame of the D and in heavy-meson chiral perturbation theory, the hadronic matrix elements are conveniently parametrized by form factors f_\perp and f_\parallel :

$$\langle K(\pi)|V_\mu|D \rangle = \sqrt{2m_D} \left[v_\mu f_\parallel^{D \rightarrow K(\pi)}(q^2) + p_{\perp\mu} f_\perp^{D \rightarrow K(\pi)}(q^2) \right], \quad (2.1)$$

¹For decays to the π^0 , there is an additional isospin factor of 1/2 on the right-hand side of Eq. (1.1).

$\approx a$ (fm)	$L^3 \times n_t$	N_{conf}	n_{src}	n_{snk}	am_l/am_s	am_{val}	κ_c
0.12	$20^3 \times 64$	2052	4	4	0.02/0.05	{0.005, 0.007,	0.1259
	$20^3 \times 64$	2259	4	4	0.01/0.05	0.01, 0.02,	0.1254
	$20^3 \times 64$	2110	4	4	0.007/0.05	0.03, 0.0415,	0.1254
	$24^3 \times 64$	2099	4	4	0.005/0.05	0.05, 0.0349}	0.1254
0.09	$28^3 \times 96$	1996	4	4	0.0124/0.031	{0.0031, 0.0047,	0.1277
	$28^3 \times 96$	1931	4	4	0.0062/0.031	0.0062,	0.1276
	$32^3 \times 96$	984	4	4	0.00465/0.031	0.0093, 0.0124,	0.1275
	$40^3 \times 96$	1015	4	4	0.0031/0.031	0.031, 0.0261}	0.1275
	$64^3 \times 96$	791	4	4	0.00155/0.031		0.1275
0.06	$48^3 \times 144$	593	4	4	0.0072/0.018	{0.0018, 0.0025,	0.1295
	$48^3 \times 144$	673	8	4	0.0036/0.018	0.0036,	0.1296
	$56^3 \times 144$	801	4	4	0.0025/0.018	0.0054, 0.0072,	0.1296
	$64^3 \times 144$	827	4	4	0.0018/0.018	0.0160, 0.0188}	0.1296
0.045	$64^3 \times 192$	801	4	4	0.0028/0.014	{0.0018, 0.0028,	0.1310
						0.0040, 0.0056, 0.0084, 0.0160, 0.0130}	

Table 1: Data on the 2+1 flavor asqtad staggered MILC ensembles for various valence masses and source times. The columns are, respectively, the lattice spacing, lattice dimensions, number of configurations, number of source times, number of 3-point sink times, light/strange sea-quark masses, valence light-quark masses, and charm hopping parameter. The analysis to date includes the full QCD points; we are considering generating data at additional source times.

where $v = p_D/m_D$, and $p_\perp = p_{K(\pi)} - (p_{K(\pi)} \cdot v)v$. f_\perp and f_\parallel can be extracted from correlator ratios. We consider

$$\bar{R}_{3,\mu}^{D \rightarrow K(\pi)}(t, T; q^2) \equiv \frac{1}{\phi_{K(\pi)\mu}} \frac{\bar{C}_{3,\mu}^{D \rightarrow K(\pi)}(t, T; \mathbf{p}_{K(\pi)})}{\sqrt{\bar{C}_2^{K(\pi)}(t; \mathbf{p}_{K(\pi)}) \bar{C}_2^D(T-t)}} \sqrt{\frac{2E_{K(\pi)}}{e^{-E_{K(\pi)}t} e^{-m_D(T-t)}}}, \quad (2.2)$$

where $\phi_{K(\pi)\mu} \equiv (1, \mathbf{p}_{K(\pi)})$, $E_{K(\pi)} = (m_D^2 + m_{K(\pi)}^2 - q^2)/(2m_D)$, and \bar{C}_3 , \bar{C}_2 are averages of correlators constructed to eliminate oscillations from opposite-parity states [4]. T and t are respectively the source-sink separation and current insertion time in the vector-current 3-points.

We use local operators for the $K(\pi)$ 2-points, smear the D interpolators with a charmonium wavefunction, and construct the currents out of light staggered and heavy clover fields [9]. For insertion times t far from 3-point source and sink, the ratios plateau to the form factors:

$$\bar{R}_{3,0}^{D \rightarrow K(\pi)} \sim f_\parallel^{D \rightarrow K(\pi)} \quad \text{and} \quad \bar{R}_{3,i}^{D \rightarrow K(\pi)} \sim f_\perp^{D \rightarrow K(\pi)} \quad \text{for } 1 \ll t \ll T. \quad (2.3)$$

The averages \bar{C}_3 require raw 3-points at successive source-sink separations T and $T+1$; to minimize our errors as a function of momentum $\mathbf{p}_{K(\pi)}$, we generate the 3-point correlators at two physical separations on each ensemble and for each set of valence quark masses [10].

We inject the 3-points and $K(\pi)$ 2-points with momenta $a\mathbf{p}_{K(\pi)}/(2\pi/L) = (0,0,0)$, $(1,0,0)$, $(1,1,0)$, $(1,1,1)$, and $(2,0,0)$ (and permutations and negatives of these components). We average the correlators over equivalent momenta (up to axis interchange) and have checked that the

wavefunction overlap factors of the $K(\pi)$ 2-points are independent of momentum. We then replace $C_2^{K(\pi)}(\mathbf{p}_{K(\pi)})$ with the less noisy $C_2^{K(\pi)}(\mathbf{0})$ in the ratios of Eq. (2.2) and use

$$\overline{R}_{3,\mu}^{D \rightarrow K(\pi)}(t, T; q^2) \equiv \frac{1}{\phi_{K(\pi)\mu}} \frac{\overline{C}_{3,\mu}^{D \rightarrow K(\pi)}(t, T; \mathbf{p}_{K(\pi)})}{\sqrt{\overline{C}_2^{K(\pi)}(t; \mathbf{0}) \overline{C}_2^D(T-t)}} \frac{E_{K(\pi)}}{e^{-E_{K(\pi)}t}} \sqrt{\frac{2e^{-m_{K(\pi)}t}}{e^{-m_D(T-t)}}}. \quad (2.4)$$

We have checked that our data obeys the continuum dispersion relation, and we substitute this relation for $E_{K(\pi)}$ in the above ratio.

To extract the masses of the $K(\pi)$ and D from the 2-point correlators, we fit to sums of exponentials with oscillating terms to account for contributions from opposite-parity states. We use the masses to construct the ratios, and we propagate the errors *via* 500 bootstraps. To extract the plateaus we fit the ratios; varying the fit function and time intervals does not significantly change the results.

The vector currents undergo renormalization. We match to the continuum by writing the renormalization factors as products of the degenerate-mass vector-current normalization factors, which we compute nonperturbatively, and correction factors whose deviations from one are perturbatively calculable [11]:

$$\langle K(\pi) | V_\mu | D \rangle = Z_{V_\mu}^{cs(d)} \langle K(\pi) | V_\mu^{\text{lat}} | D \rangle, \quad Z_{V_\mu}^{cs(d)} = \rho_{V_\mu}^{cs(d)} \sqrt{Z_{V_4}^{cc} Z_{V_4}^{ss(dd)}}. \quad (2.5)$$

We blind the analysis by introducing an offset in ρ .

After operator renormalization, the results for the form factors on all ensembles and for all combinations of valence masses and momenta are simultaneously fit to staggered chiral perturbation theory (S χ PT) [12]. Fits to SU(3) S χ PT are shown in Fig. 1. The data are for the $D \rightarrow \pi$ decay on a subset of the ensembles of Table 1: the four coarse ($a \approx 0.12$ fm) ensembles, four of the fine ($a \approx 0.09$ fm) ensembles (excluding the $0.05m_s$ ensemble), and three of the superfine ($a \approx 0.06$ fm) ensembles (excluding the $0.14m_s$ ensemble). Data with momenta up through $\mathbf{p}_\pi = (1, 1, 0)$ are included in the fits.² The fit function includes leading chiral logarithms (NLO loops) and analytic terms through NNLO.

The SU(3) S χ PT fits for $f_\perp^{D \rightarrow \pi}$ and $f_\perp^{D \rightarrow K}$ are good, much better than SU(3) S χ PT fits for $f_\parallel^{D \rightarrow \pi}$ and $f_\parallel^{D \rightarrow K}$. As exemplified in Fig. 1, fits of $f_\parallel^{D \rightarrow \pi}$ data to SU(3) S χ PT are marginal in quality. We understand this behavior in terms of the features of the χ PT description of the energy dependence of the form factors.

The pole from the resonance dominates the energy dependence of f_\perp , but the χ PT expressions for f_\parallel contain no pole, and the fits suffer. The fit quality for f_\parallel may also reflect the limitations of χ PT. For energies comparable to the chiral symmetry breaking scale, $E_{K(\pi)} \sim \Lambda_{\chi\text{SB}}$, we expect the χ PT description of the energy dependence to break down. The largest-momentum data in fits to date have $\mathbf{p}_{K(\pi)} = (1, 1, 0)$, which corresponds to $E_\pi \sim \Lambda_{\chi\text{SB}}$; on the coarse ensembles, $\mathbf{p}_\pi = (1, 1, 1)$ corresponds to energies $E_\pi \gtrsim \Lambda_{\chi\text{SB}}$.

SU(3) S χ PT fits for $f_\parallel^{D \rightarrow K}$ support the idea that the χ PT description of the energy dependence of f_\parallel is breaking down. For the same momenta, the energies E_K are larger than the energies E_π , the

²Hereafter all momenta are given in units of $2\pi/(aL)$ unless otherwise specified.

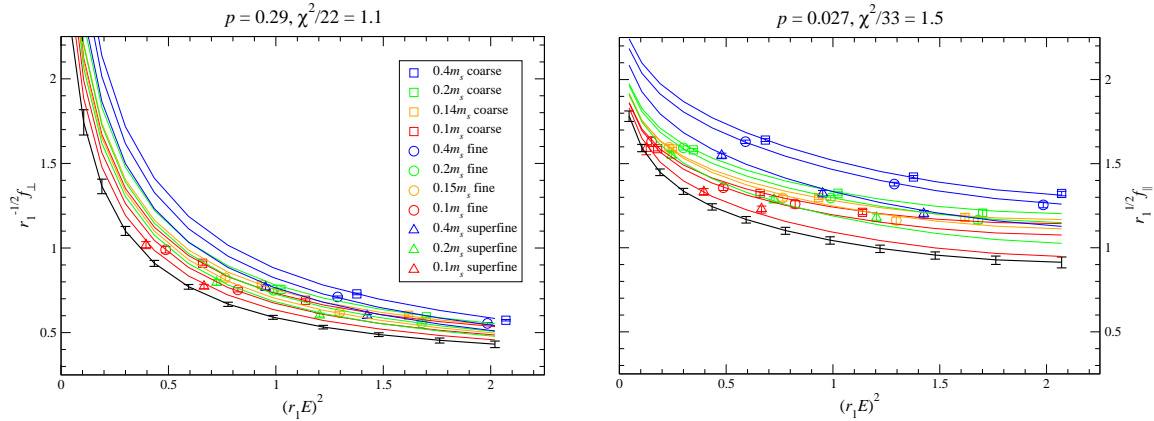


Figure 1: Fits of $D \rightarrow \pi$ data to SU(3) $S\chi$ PT; the legend applies to both plots. Included are full QCD data from 11 ensembles at three lattice spacings and four light-quark masses. The fit quality for $f_{\perp}^{D \rightarrow \pi}$ (left) is good, but the fit quality for $f_{\parallel}^{D \rightarrow \pi}$ is marginal (right).

χ PT expansion breaks down for smaller momenta, and fits for $f_{\parallel}^{D \rightarrow K}$ should be worse than fits for $f_{\parallel}^{D \rightarrow \pi}$. In fact, SU(3) $S\chi$ PT fits for $f_{\parallel}^{D \rightarrow K}$ have unacceptably small p -values ($p < 10^{-3}$).

To better parametrize the f_{\parallel} data, we are investigating alternative fit functions, including SU(2) $S\chi$ PT. An improved treatment of the energy dependence of f_{\parallel} would be especially desirable for adding data at higher momenta. (Cf. Sec. 4.) At the same time, f_{\perp} dominates the desired form factor f_{+} , and SU(3) $S\chi$ PT fits for $f_{\perp}^{D \rightarrow \pi}$ and $f_{\perp}^{D \rightarrow K}$ are good. Any model dependence in $f_{+}^{D \rightarrow \pi}$ introduced by the χ PT description of the energy dependence of $f_{\parallel}^{D \rightarrow \pi}$ is probably small. We therefore proceed to compare the shape of the form factor $f_{+}^{D \rightarrow \pi}$ obtained from the fits shown in Fig. 1 to the shape measured by CLEO.

3. Comparison of lattice QCD and experiment

If lattice calculations are to be combined with experimental results, the lattice and experimental results must be consistent. Experiments measure shapes of form factors but cannot fix their normalizations without the CKM matrix elements (Eq. (1.1)). For $D \rightarrow K(\pi)\ell\nu$, experiments and lattice calculations access the same q^2 region, and comparisons of the lattice and experimental form factor shapes provide stringent tests of lattice QCD.

In Fig. 2 we overlay our calculated $f_{+}^{D \rightarrow \pi}$, normalized to the point $\tilde{q}^2 = 0.15 \text{ GeV}^2$, with the same ratio from CLEO [3]. The orange (dark grey) error band is the statistical error obtained by including data from two coarse and three fine ensembles [13]. The yellow (light grey) error band is the statistical error obtained by including data from the 11 ensembles of Fig. 1. The curves are from SU(3) $S\chi$ PT, and the errors are from 500 bootstraps. The errors scale as naively expected. The form factor shapes from CLEO and the lattice calculation agree well.

4. Projected errors

To conservatively estimate our errors, we begin with the error budget of our $B \rightarrow \pi\ell\nu$ calculation [4]. At $q^2 = 0$ naive scaling to the full QCD data set of Table 1 gives a statistical error of 4.2%

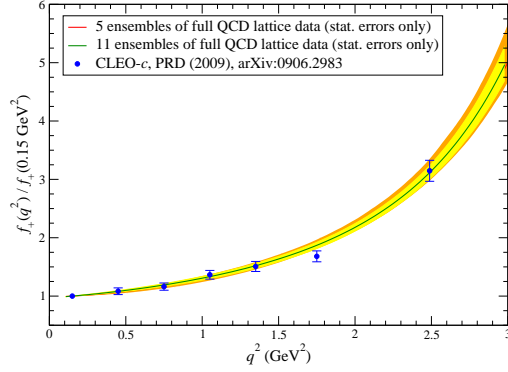


Figure 2: Overlay of the ratio $f_+^{D \rightarrow \pi}(q^2)/f_+^{D \rightarrow \pi}(\tilde{q}^2)$ from the lattice (curves and error bands) and CLEO (blue points) [3]. The larger lattice errors are from 5 ensembles, and the smaller are from 11 ensembles. The form factor shapes from CLEO and the lattice agree; the errors scale as expected.

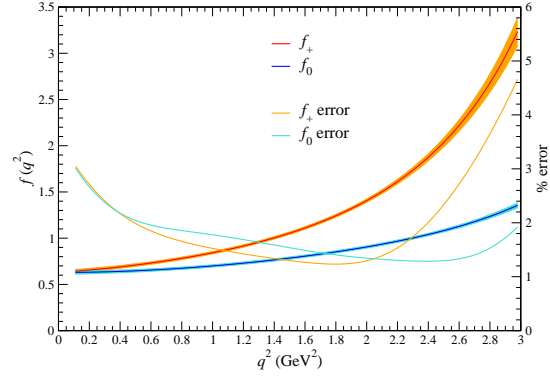


Figure 3: The form factors $f_+^{D \rightarrow \pi}(q^2)$ and $f_0^{D \rightarrow \pi}(q^2)$ and their statistical errors. The curves are from $S\chi PT$, and the errors are from the Hessian. The percent errors are plotted against the right-hand axis. The larger errors at small q^2 probably reflect excluded data at corresponding momenta on the finer, more chiral ensembles.

and an error from the degenerate-mass vector-current normalization factors of 0.6%. Updating the heavy-quark and ρ -factor power counting estimates to account for the ultrafine data gives errors of 2.5% and 0.5%, respectively. For the remaining errors we adopt our previous estimates [10]. This leads to a total error of 6.1% for $f_+^{D \rightarrow K(\pi)}(0)$. However, this estimate may be overly conservative. In Fig. 3 we plot the form factors (with the ρ -factors set to one) $f_+^{D \rightarrow \pi}(q^2)$ and $f_0^{D \rightarrow \pi}(q^2)$ and their statistical errors as functions of q^2 . The data are from the 11 ensembles of Fig. 1.

The errors at q_{\max}^2 are much smaller for f_0 than for f_+ because f_+ (f_0) is dominated by f_\perp (f_\parallel), and we have data for f_\perp (f_\parallel) for $|\mathbf{p}_\pi| \geq 0.33 \text{ GeV} \leftrightarrow q^2 \leq 2.0 \text{ GeV}^2$ ($|\mathbf{p}_\pi| \geq 0 \leftrightarrow q^2 \leq q_{\max}^2$). As q^2 decreases, the errors reflect the addition of data and the hyperbolic behavior of the form factors; the errors in f_+ (f_0) grow approximately linearly in the region $1.6 \text{ GeV}^2 \gtrsim q^2 \gtrsim 0.8 \text{ GeV}^2$ ($2.0 \text{ GeV}^2 \gtrsim q^2 \gtrsim 0.6 \text{ GeV}^2$). The largest momentum of data in the fit is $\mathbf{p}_\pi = (1, 1, 0)$, which corresponds to $q^2 \in [0.43, 1.58] \text{ GeV}^2$ on the ensembles with $m_l \leq 0.2m_s$, and to $q^2 \in [0.69, 1.58] \text{ GeV}^2$ on the superfine ensembles. Without data points below $q^2 = 0.43 \text{ GeV}^2$ on the finer, more chiral ensembles, the errors increase rapidly as q^2 decreases in the region $0.3 \text{ GeV}^2 > q^2 > 0$.

Extrapolating the curve for the statistical error in f_+ to $q^2 = 0$, the error grows to about 3.6%, somewhat smaller than that expected from naive scaling to the entire full QCD data set. Including data at smaller q^2 would allow interpolation to $q^2 = 0$ and might improve the errors significantly. We can appreciate the potential of the additional data by linearly extrapolating the curve for the error in f_+ for $q^2 \in [0.8, 1.6] \text{ GeV}^2$ to $q^2 = 0$. The resulting expected error is about 2.0%. Adding a statistical error of 3.6% (2.0%) to our systematics yields a total error of 5.7% (4.8%). Corresponding error budgets are in Table 2. We conclude that including data at momenta greater than $\mathbf{p}_{K(\pi)} = (1, 1, 0)$ may improve the error in $f_+(0)$ to better than 5%. This prospect further motivates us to consider alternatives to $SU(3) S\chi PT$ for describing the energy dependence of f_\parallel at small q^2 . (Cf. the last paragraph of Sec. 2.)

Computations were carried out with resources provided by the USQCD Collaboration, Ar-

	Stat.	g_π	r_1	\hat{m}	m_s	κ_c	p_π	HQ	Z_V	ρ	FV	Sys.	Tot.
(a)	3.6	2.9	1.4	0.3	1.3	0.2	0.1	2.5	0.6	0.5	0.5	4.4	5.7
(b)	2.0	2.9	1.4	0.3	1.3	0.2	0.1	2.5	0.6	0.5	0.5	4.4	4.8

Table 2: Projected error budgets for the form factors at $q^2 = 0$, assuming we (a) exclude data at momenta greater than $\mathbf{p}_{K(\pi)} = (1, 1, 0)$ and (b) include data at momenta greater than $\mathbf{p}_{K(\pi)} = (1, 1, 0)$. Errors are due to limited statistics and the truncation of $S\chi$ PT; uncertainties in the $D^*D\pi$ coupling, scale, average up-down quark mass, strange quark mass, and charm hopping parameter; momentum-dependent discretization effects of the light quarks and gluons; heavy-quark discretization effects; uncertainties in the matching factors Z_V and ρ ; and finite volume effects. The last two entries are the total systematics and total error.

gonne Leadership Computing Facility, and National Energy Research Scientific Computing Center, which are funded by the Office of Science of the U.S. DOE; and with resources provided by the National Institute for Computational Science, Pittsburgh Supercomputer Center, San Diego Supercomputer Center, and Texas Advanced Computing Center, which are funded through the National Science Foundation’s Teragrid/XSEDE Program. This work was supported in part by the U.S. DOE under grant Nos. DE-FG02-91ER40661 (S.G.), No. DE-FG02-91ER40677 (R.D.J., A.X.K.). This manuscript was co-authored by employees of Brookhaven Science Associates, LLC, under Contract No. DE-AC02-98CH10886 with the U.S. DOE. R.S.V. acknowledges support from BNL via the Goldhaber Distinguished Fellowship. J.A.B. is supported by the Creative Research Initiatives program (3348-20090015) of the NRF grant funded by the Korean government (MEST). Fermilab is operated by Fermi Research Alliance, LLC, under Contract No. DE-AC02-07CH11359 with the U.S. DOE.

References

- [1] J. Charles *et al.* [CKMfitter], Phys. Rev. D **84**, 033005 (2011)
- [2] K. Nakamura *et al.* [PDG], J. Phys. G **37**, 075021 (2010)
- [3] D. Besson *et al.* [CLEO], Phys. Rev. D **80**, 032005 (2009)
- [4] J. Bailey *et al.* [Fermilab Lattice and MILC], Phys. Rev. D **79**, 054507 (2009)
- [5] R. Zhou *et al.* [Fermilab Lattice and MILC], arXiv:1111.0981 [hep-lat]
- [6] K. Orginos, D. Toussaint and R. L. Sugar [MILC], Phys. Rev. D **60**, 054503 (1999), and references therein.
- [7] A. X. El-Khadra, A. S. Kronfeld and P. B. Mackenzie, Phys. Rev. D **55**, 3933 (1997), A. S. Kronfeld, *ibid.* **62**, 014505 (2000)
- [8] C. W. Bernard *et al.* [MILC], Phys. Rev. D **58**, 014503 (1998), and references therein.
- [9] M. Wingate *et al.* [HPQCD], Phys. Rev. D **67**, 054505 (2003)
- [10] J. A. Bailey *et al.* [Fermilab Lattice and MILC], PoS **LAT2009**, 250 (2009)
- [11] A. X. El-Khadra *et al.*, Phys. Rev. D **64**, 014502 (2001)
- [12] C. Aubin and C. Bernard, Phys. Rev. D **76**, 014002 (2007)
- [13] J. A. Bailey *et al.* [Fermilab Lattice and MILC], PoS **LATTICE2010**, 306 (2010)